PRAMANA
— journal of
physics

Vol. 74, No. 5
May 2010
pp. 719–729

Beam-induced radiation in the compact muon solenoid tracker at the Large Hadron Collider

A P SINGH[1,*], P C BHAT[2], N V MOKHOV[2] and S BERI[1]
[1]Department of Physics, Panjab University, Chandigarh 160 014, India
[2]Fermi National Accelerator Laboratory, Batavia, IL 60510, USA
[*]Corresponding author. E-mail: anil79@fnal.gov

MS received 22 September 2009; revised 24 December 2009; accepted 13 January 2010

Abstract. The intense radiation environment at the Large Hadron Collider, CERN at a design energy of $\sqrt{s} = 14$ TeV and a luminosity of 10^{34} cm^{-2} s^{-1} poses unprecedented challenges for safe operation and performance quality of the silicon tracker detectors in the CMS and ATLAS experiments. The silicon trackers are crucial for the physics at the LHC experiments, and the inner layers, being situated only a few centimeters from the interaction point, are most vulnerable to beam-induced radiation. We have recently carried out extensive Monte Carlo simulation studies using MARS program to estimate particle fluxes and radiation dose in the CMS silicon pixel and strip trackers from proton–proton collisions at $\sqrt{s} = 14$ TeV and from machine-induced background such as beam–gas interactions and beam halo. We will present results on radiation dose, particle fluxes and spectra from these studies and discuss implications for radiation damage and performance of the CMS silicon tracker detectors.

Keywords. Compact muon solenoid; tracker; beam radiation; dose; fluences.

PACS Nos 13.85.-t; 13.74.-n

1. Introduction

The compact muon solenoid (CMS) detector has to operate in the unprecedented radiation environment of high energy ($\sqrt{s} = 14$ TeV) and high luminosity (design of 10^{34} cm^{-2} s^{-1}) proton–proton (*pp*) collisions at the Large Hadron Collider at CERN. This will lead to very high particle fluxes and energy deposition in detector components which may cause serious damage, especially in the silicon tracker that is physically very close to the interaction point (IP) [1]. Radiation damage could be either bulk damage, i.e., changes in the lattice structure of Si, or surface damage. The consequences would be increased leakage current, increase in the required biasing voltage and/or reduced signal collection efficiency.

Apart from the fluxes originating from *pp* collisions, machine-induced backgrounds (MIB) and beam accidents are also of concern. The MIB arise due to interactions of the beam particles with the beam line elements and molecules of residual gas in the beam pipe vacuum. We have formally divided the machine-induced backgrounds according to the source of its origin.

- Protons escaping the betatron and momentum cleaning insertions and intercepted by beam collimators producing secondaries. These 'cleaning tails from collimators' are also called beam halo.
- Beam–gas interactions in the straight section and arcs in the LHC, upstream of the IP.

In this report we provide some preliminary results from simulations carried out for *pp* interaction scenario and for beam halo and beam–gas backgrounds, with emphasis on the tracker region of the detector.

2. The LHC and the CMS experiment

The Large Hadron Collider (LHC) at CERN is housed in a tunnel of 27 km circumference and at a depth underground varying from 50 to 175 m, straddling the borders of France and Switzerland. The LHC is built to collide two proton beams of a maximum energy of 7 TeV each and instantaneous luminosity of 10^{34} cm^{-2} s^{-1}. The LHC has about 1232 dipoles and 400 quadrupoles and 7000 other optical correction elements in its lattice. It is a very complex machine with the superconducting magnets operating at a liquid helium temperature of 1.9 K. Figure 1 shows a schematic view of LHC ring. Some of the salient parameters of the LHC are shown in table 1. The CMS detector shown in figure 2 is one of the two general purpose collider experiments designed and built to study high p_{T} physics. The detector comprises of tracking system made of silicon pixel and strip detectors, electromagnetic calorimeter (ECAL) and hadronic calorimeter (HCAL) housed inside 4 T magnetic field of a superconducting solenoid and a muon system (MS). The silicon-based pixel and inner tracker lie very close to the interaction point.

Each beam in the LHC will have 2808 proton bunches with a bunch spacing of about 25 ns which means that there will be 4×10^7 bunch crossings per second. Collision rate is calculated by multiplying instantaneous luminosity, with inclusive proton–proton interaction cross-section at 14 TeV centre of mass energy. Using 80 mb for *pp* cross-section the collision rate turns out to be 8×10^8 s^{-1}. This rate is used in the scaling of simulation results to estimate the particle fluences in various detector components.

After an unsuccessful attempt in 2008, beam commissioning efforts were re-ignited in November 2009. First collisions in CMS at 900 GeV and 2.36 TeV

Table 1. Nominal beam parameters at LHC [2]. Here ϵ_{T} stands for transverse emittance, ϵ_{L} (inj.) and (coll.) for longitudnal emittances at injection and collison. BL$_{\mathrm{rms}}$ is the rms bunch length.

Bunches per beam	Bunch spacing	Protons per bunch	ϵ_{T}	ϵ_{L} (inj.)	ϵ_{L} (coll.)	BL$_{\mathrm{rms}}$ (inj.)	BL$_{\mathrm{rms}}$ (top energy)
2808	25 ns	1.1×10^{11}	3.75 μm	1.00 eV s	2.5 eV s	17.50 cm	7.7 cm

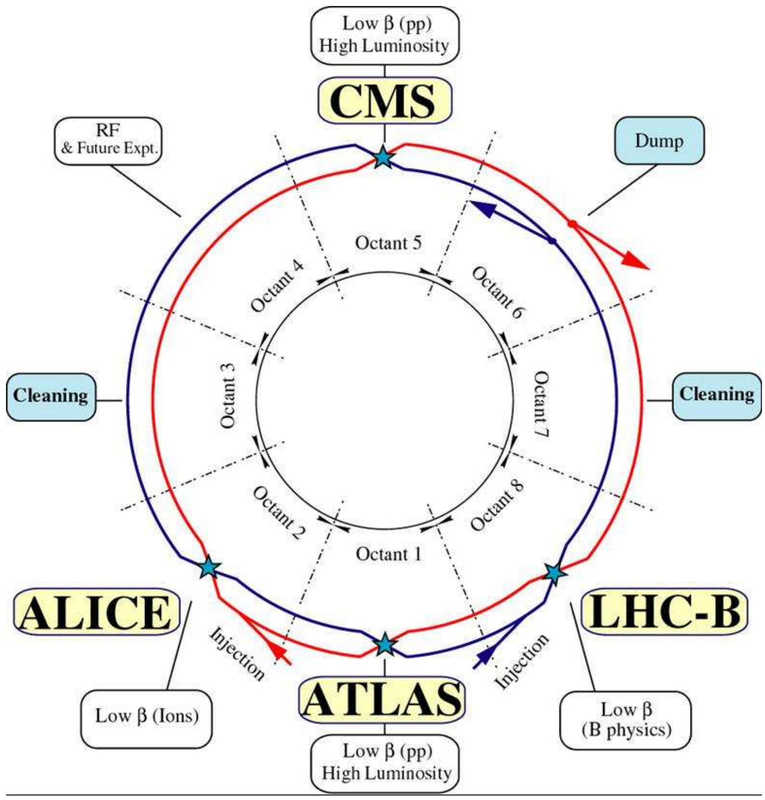

Figure 1. A schematic view of LHC ring showing the locations of all the interaction points. CMS and ATLAS are two general purpose experiments while ALICE, LHC-B are dedicated for heavy-ion collisions and b-physics respectively. There are two cleaning insertions on the ring, one for amplitude cleaning and the other for momentum cleaning.

centre of mass energy were observed in the first half of December 2009. The 2009 LHC run did come to an end on 16 December 2009. Machine will be restarted in February 2010 and the beam energies would be ramped up to 3.5 TeV thus enabling collisions with 7 TeV centre of mass energy. Given the energy regime and luminosity, studying the radiation environment and it's implications in terms of detector performance can hardly be over-estimated. Although the nominal luminosity and collision energy assumed in this work would take some more time for being achieved, the current study allows us to set conservative benchmarks for studying the expected radiation environment.

3. MARS Monte Carlo simulations

The radiation damage and the background rates in the detectors are mainly determined by the low-energy phenomena. At the LHC, high beam energy and high

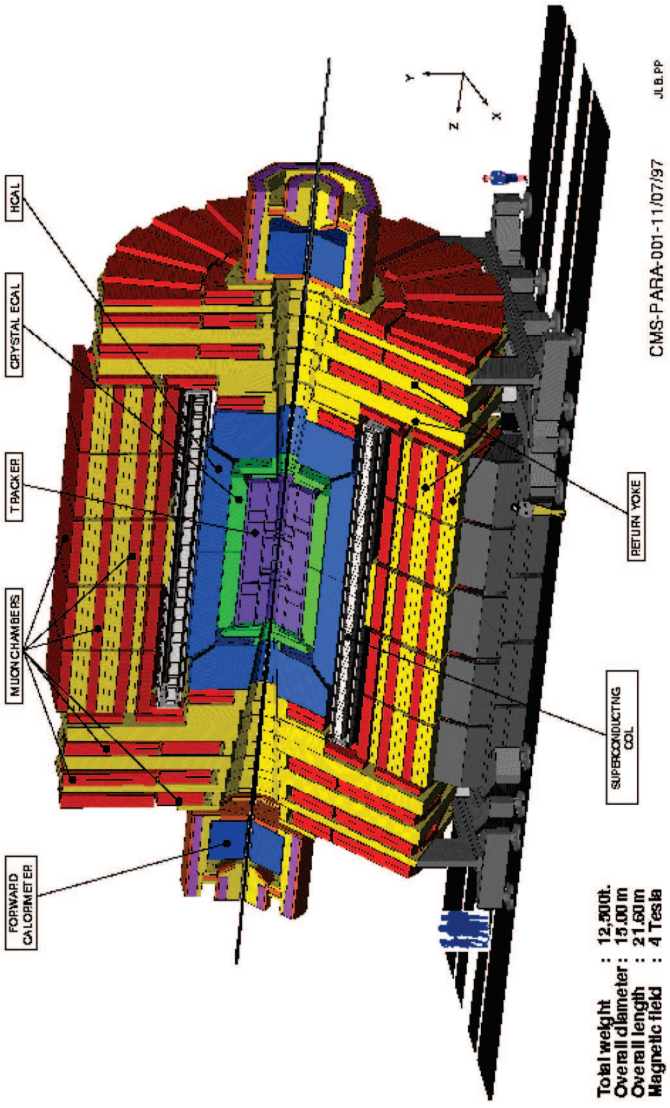

Figure 2. A schematic view of CMS detector showing various detector regions. Innermost layers (violet) are the Si tracker and pixel detectors, followed by the electromagnetic (green) and hadronic calorimeters (blue), superconducting coil (grey), and muon system. Muons system consists of muon stations (red) interspersed between the yoke layers (yellow).

luminosity cause intense cascades, leading to the production of a very large number of low-energy particles. Hence, dedicated studies for the radiation environment require proper treatment of low-energy interactions of all particles. Most simulations for the detector performance evaluation do not deal with low-energy interactions. So a study with implications for the detector damage and machine backgrounds has to be carried out in a specialized framework. MARS Monte Carlo software provides this special framework. MARS was developed 30 years ago, for fast inclusive as well as exclusive simulation of the 3D hadronic cascades, electromagnetic cascades, transport of the low-energy neutrons, photons and muons through the various accelerator, detector and shielding components [3,4]. The CMS detector geometry was modelled using the MCNP geometry package suitably interfaced with MARS. The detector model has cylindrical symmetry about the beam axis, and includes active detector layers along with the major support structures.

The fluxes and the dose were scored in various parts of the CMS detector. We define flux as the track length of particles per unit volume per unit time. Absorbed dose in a material segment is defined as energy deposited per unit mass and is expressed here in Grey (1 Gy = J/kg). Although the reactions taking place inside a semiconductor may be complex, the evolution of macroscopic characteristics may be described rather simply by NIEL hypothesis. According to this, the damage in the material to first order depends only on the nonionizing component of dose (NIEL) and not on the type of radiation field. This allows to sum the fluxes due to different particle types weighted according to the respective damage functions,

$$\Phi_{\rm NIEL} = \Phi_p + \Phi_\pi + 0.5\Phi_\mu + \Phi_{n>0.1\,\rm MeV} + 0.01\Phi_\gamma.$$

NIEL scales with the interaction cross-section for different particle types in the matter, and this decides the numerical coefficients for different particle types.

4. *pp* Scenario: Dose and fluxes in the tracker

We generated 13,000 minimum bias events at $\sqrt{s} = 14$ TeV with DPMJET-II [5] event generator which uses dual parton model to describe *pp* collisions. This provided a source of about 1.5 million particles (four-vectors and particle ID) to be fed into MARS code, for detailed shower simulation and tracking. We present the results on the dose and fluxes in the following figures and tables.

As already stated, we expect large flux of particles in the tracker region due to its physical proximity to the collision point. Such an intense radiation environment may induce the formation of permanent defects in the lattice. These are actually recombination centres acting as electron or hole traps depending on their level inside the band gap. Macroscopically they would lead to enhanced leakage current, modify the depletion voltage and diminish the charge collection efficiency. Figure 3 shows the dose in the pixel and Si tracker layers as a function of distance from the interaction point along the beam axis z. No appreciable z dependence of dose is seen in the tracker volume. The radial dependences of the dose are shown in figure 4. In the absence of a magnetic field, one would expect an inverse square dependence of fluxes and dose on the radial distance. In this case, because of the magnetic field that bends the low-energy particles more, the radial dependence is

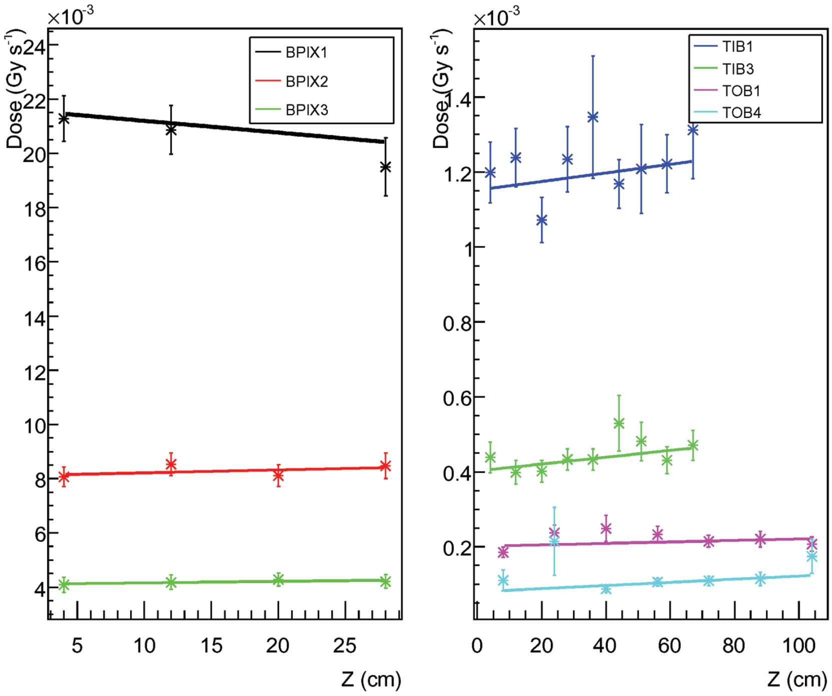

Figure 3. Plots showing the variation of dose (y-axis) with horizontal distance (x-axis) from the nominal interaction point for pixel (left) and tracker layers (right).

harder than the inverse square. For inner tracker layers, it is $r^{-1.76}$, and $r^{-1.9}$ in the outer tracker region.

The fluxes of particles in various tracker layers are shown in table 2. It can be seen that the charged hadron flux dominates at smaller radii but falls much faster with radii than the neutral hadron flux which is more or less uniform in the outer tracker region. This is due to the neutron backscattering by the material in the electromagnetic calorimeters (albedo neutrons). It is to be noted that fluxes upto a radii of about 50 cm are dominated by the secondaries coming from the IP, whereas in the outer regions albedo neutrons dominate. Similarly, the albedo effect increases towards the outer tracker endcaps. The potential damage by albedo neutrons can be lowered significantly by having good shielding, and since the neutrons below 1 MeV have only vanishing contribution towards the dose, we need material just enough to slow down the neutrons below 1 MeV. Since elastic interactions of the neutrons with hydrogen atoms can serve this purpose well, the CMS has opted for polyethylene shielding which is easy to handle and machine. Assuming nominal operation for 0.5×10^7 s year^{-1} the annual fluences are calculated from table 2. They are of the order of 10^{14} for the pixel region and 10^{11} for the inner tracker region. Silicon pixel and strip detectors have been shown to remain functional at fluences beyond 1×10^{15} cm^{-2} for minimum ionizing protons [6]. So we expect the pixel detectors to survive less than one year of nominal operation and inner tracker

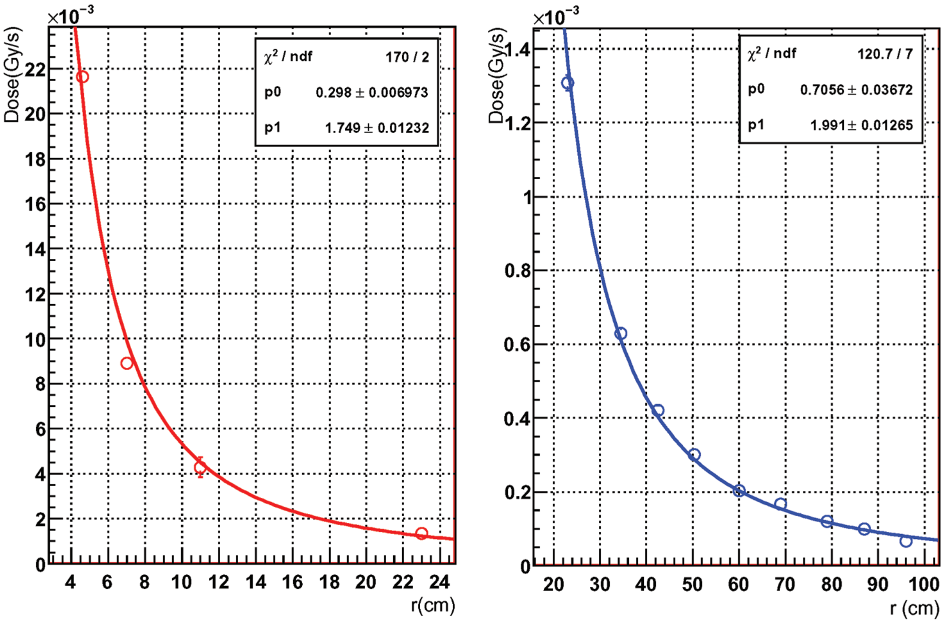

Figure 4. Plots showing the variation of dose (y-axis) with the radial distance from the beam axis (x-axis) in the inner (left) and outer (right) tracker layers. Dose is seen to scale as $r^{-1.76}$ in the inner layers and $r^{-1.98}$ in outer layers.

Table 2. Fluences in barrel Si tracker detector (10^5 cm^{-2} s^{-1}). We can see that neutron fluxes are almost uniform in the outer tracker region because of albedo neutrons. The quoted numbers for radii are the ones from MARS CMS Model implemented for the current study.

Detector layer	Radius (cm)	Charged hadrons	Neutral hadrons	Charged EMS	Muons
BPIX1	4.1	493 ± 3.45	64.9 ± 0.45	88.5 ± 0.61	9.21 ± 0.03
BPIX2	7.2	181 ± 1.62	26.5 ± 0.22	36.6 ± 0.32	5.45 ± 0.26
BPIX3	11.1	85 ± 0.80	12.1 ± 0.12	14.4 ± 0.14	4.03 ± 0.02
TIB1	23.4	24.4 ± 0.39	6.80 ± 0.10	7.37 ± 0.11	2.77 ± 0.03
TIB2	34.5	11.9 ± 0.26	5.22 ± 0.12	4.40 ± 0.09	1.44 ± 0.26
TIB3	42.3	7.88 ± 0.19	4.64 ± 0.11	3.03 ± 0.07	0.90 ± 0.02
TIB4	50.1	5.24 ± 1.09	3.96 ± 0.07	2.40 ± 0.04	0.63 ± 0.10
TOB1	61.0	3.43 ± 1.07	3.88 ± 0.85	1.77 ± 0.35	0.55 ± 0.06
TOB2	69.0	2.37 ± 1.04	3.69 ± 0.06	1.52 ± 0.02	0.22 ± 0.03
TOB3	78.0	1.69 ± 0.02	3.49 ± 0.04	1.21 ± 0.01	0.11 ± 0.26
TOB4	86.0	1.13 ± 0.01	3.48 ± 0.04	0.09 ± 0.01	0.08 ± 0.02
TOB5	96.0	0.76 ± 1.16	3.34 ± 0.73	0.79 ± 0.17	0.05 ± 0.10
TOB6	108.0	0.46 ± 1.02	3.39 ± 0.20	0.59 ± 0.03	0.04 ± 0.06

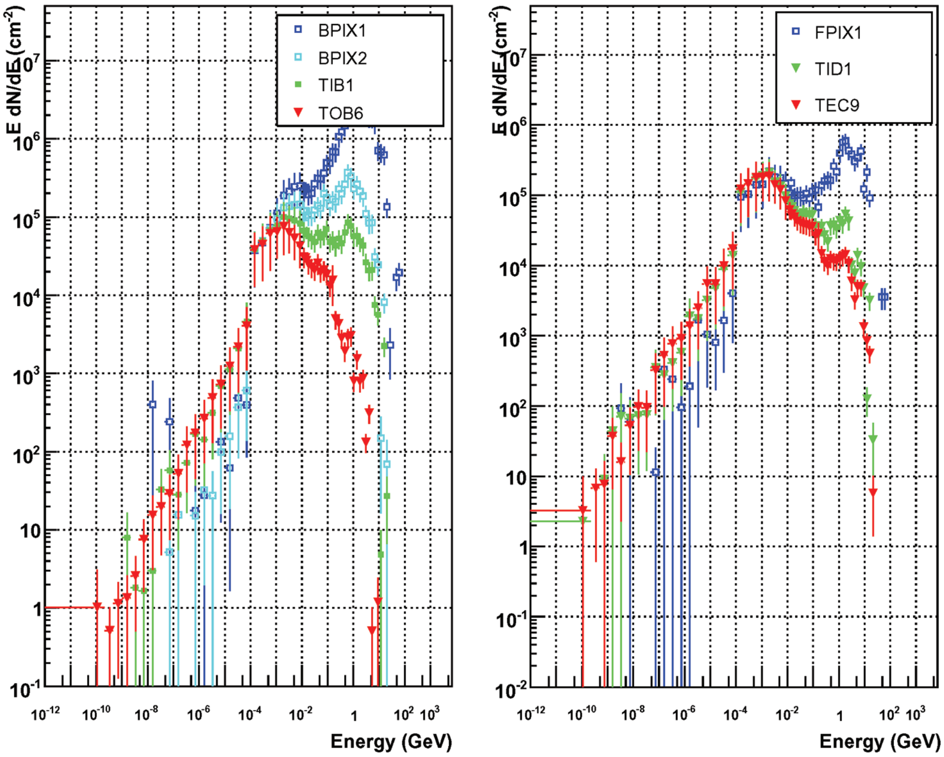

Figure 5. Neutral hadron spectra in the tracker: barrel layers (left) and endcaps (right). Spectrum is hardest in the innermost pixel layers and softens as we go to higher radii. We can see local maxima at 1 MeV, which is the evaporation peak. Also quasielastic hump at 60–70 MeV is seen.

layers to survive about seven to eight years. Detailed results for the outer detector components such as ECAL, HCAL and muon chambers have also been obtained and compiled. They will be reported in future.

5. Machine-induced backgrounds

The machine-induced backgrounds (MIB) depend on a large number of parameters like machine optics, cleaning inefficiencies, residual gas pressure and the location of possible source points with respect to the experiment's interaction point. As pointed out before, the MIB would be a minor source of background during normal operational conditions. Generically speaking MIB originate from losses of the beam particles [7] around the machine ring. Even in fully tuned operations, such beam losses lead to the formation of a beam halo. The halo particles may then lead to secondary showers by interacting with limiting aperture elements. We have been conducting extensive studies for MIB expected in the CMS detector. Here we briefly discuss results for the two major sources.

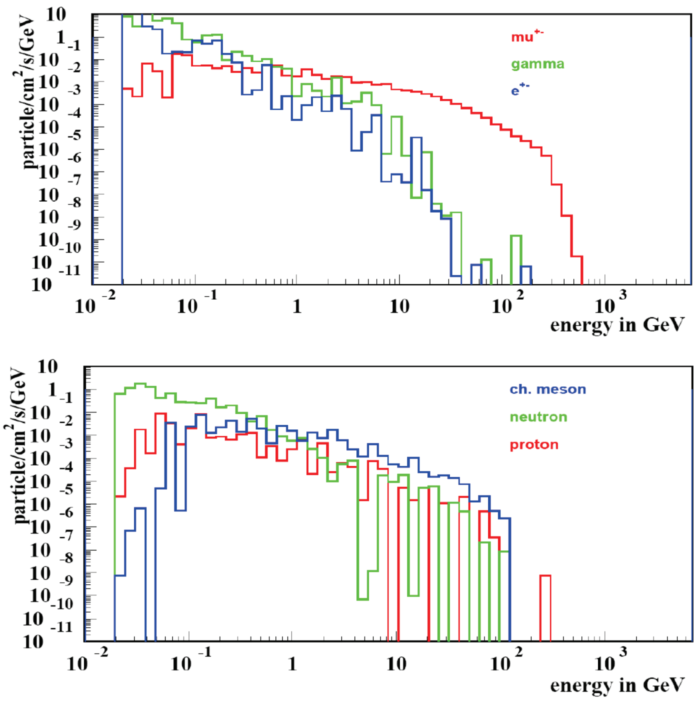

Figure 6. Energy spectra for charged and neutral EM particles, muons (top) and charged, neutral hadrons (bottom), at $z = 22.6$ cm from IP-5 in $1.7 < r < 100$ cm region for tertiary beam halo.

- Collimation tails [8] arise due to the protons that escape betatron and momentum cleaning insertions at IP7 and IP3 respectively and are subsequently intercepted by tertiary collimators upstream of IP5. Because of the geometry close to IP5, most of the protons coming from IP3 and IP7 would be lost in the low-beta quadrupole triplets just outside the detector, if not intercepted by the TCT.

  A sample source of collimator tails has been generated consisting of particles at 22.6 m from the interaction point. This is generated by MARS simulations in an ideal machine at 7 TeV beam energy, with $\beta^* = 0.55$ m for the high-luminosity insertions and processing the contributions from the betatron cleaning. The contributions from the momentum cleaning are estimated to be substantially lower and hence neglected. Figure 6 shows energy spectra at $z = 22.6$ m from IP for beam halo.

- Products of the beam–gas interaction in straight sections and arcs that escape interception by the collimation system have a very good chance of ending up in the collider detectors. The main process in beam–gas interactions is multiple Coulomb scattering [8] which leads to the growth of emittance due to slow diffusion of the protons from the beam core. After several turns these particles acquire large betatron amplitudes and are intercepted by the main

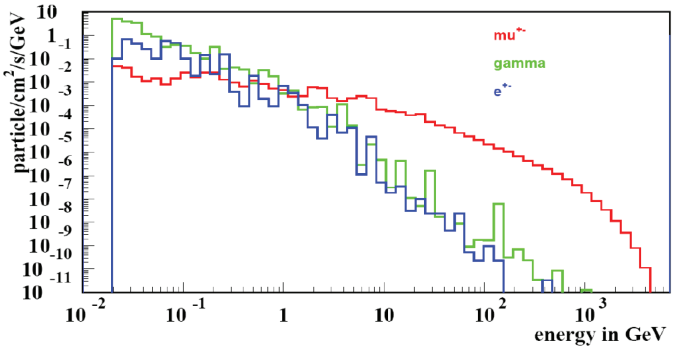

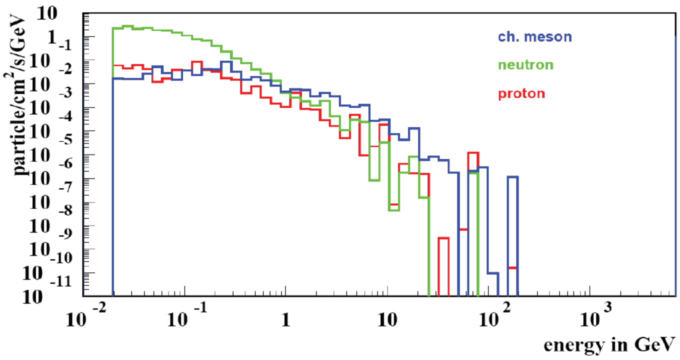

Figure 7. Energy spectra for charged and neutral EM particles, muons (top) and charged, neutral hadrons (bottom), at $z = 22.6$ cm from IP-5 in $1.7 < r < 100$ cm region for beam–gas interactions.

collimators. Similar behaviour is seen for small angle elastic nuclear scattering, inelastic nuclear interactions – leading nucleon and other secondaries are generated at large angles and thus they are lost within hundreds, if not tens, of meters of the LHC ring. Figures 6 and 7, taken from [8] show energy spectra of particles at $z = 22.6$ m from IP for beam–gas background.

6. Summary

Monte Carlo simulations of the radiation environment in CMS have been done using MARS code for 14 TeV *pp* interaction scenario of the LHC, and for beam halo and beam–gas backgrounds. In this report, we have particularly focussed on results from *pp* simulations in the CMS silicon pixel and strip trackers. The dose and fluxes in the tracker for *pp* scenario are in general agreement with the results from studies done a decade ago with FLUKA. Preliminary study of machine-induced backgrounds shows that they are several orders of magnitude lower at CMS, under normal conditions. Detailed reports of the extensive simulation studies of *pp* and the machine-induced backgrounds will be reported elsewhere.

References

[1] Mika Huhinten, *Radiation environment simulations for CMS detector*, CERN CMS TN/95-198
[2] http://ab-div.web.cern.ch/ab-div/publications/LHC-DesignReport.html
[3] N V Mokhov, *The MARS code system user's guide*, Fermilab-FN-628 (1995)
[4] N V Mokhov, *Status of Mars code*, Fermilab-conf-03/053 (2004)
[5] J Ranft, *Phys. Rev.* **D51**, 64 (1995)
[6] Particle data group, Review of particle physics, *J. Phys.* **G284**, 285
[7] N V Mokhov, *Beam collimation at hadron colliders*, *AIP Conf. Proc.* 693 (2003)
[8] N V Mokhov and T Weiler, Machine induced backgrounds: Their origin and loads on ATLAS/CMS, FERMILAB-CONF-08-147-APC